ELSEVIER

International Journal of Mass Spectrometry 210/211 (2001) 21–30

International Journal of Mass Spectrometry

www.elsevier.com/locate/ijms

Excitation processes in alkali-cationized esters: a molecular orbital study

I. Vedernikova[a], M. Claeys[a,*], D.R. Salahub[b,c], M.E. Casida[b]

[a]*Department of Pharmaceutical Sciences, University of Antwerp (UIA), Universiteitsplein 1, 2610 Antwerp, Belgium*
[b]*Centre de Recherche en Calcul Appliqué (CERCA), 5160 Boulevard Decarie, Montréal, Québec H3X 2H9, Canada*
[c]*Department of Chemistry, University of Montréal, C.P. 6128, Succ. Centreville, Montréal, Québec H3C3J7, Canada*

Received 10 November 2000; accepted 10 February 2001

Abstract

Theoretical calculations on Li^+ and Na^+ cationized methyl and *n*-butyl acetate, and methyl butyrate, were performed in order to explain the very different fragmentation behavior of Li^+ and Na^+ cationized fatty acid *n*-butyl esters in low-energy collisional activation. Li^+ cationized *n*-butyl palmitate shows loss of 1-butene from the ester moiety, while the corresponding Na^+ adduct does not reveal this loss. This elimination of 1-butene can be regarded as a McLafferty-type rearrangement and since it bears similarity with the well-known Norrish II photochemical rearrangement of ketones, involving an intramolecular γ-hydrogen transfer due to an excitation of the carbonyl bond, we postulated that an excitation of the Li^+ cationized ester carbonyl bond in Li^+ adducts of fatty acid *n*-butyl esters is the trigger for the loss of 1-butene in low-energy collisional activation. For the theoretical calculations using density-functional theory was considered because excited states can be treated by this approach. The results obtained on Li^+ and Na^+ cationized methyl and *n*-butyl acetate and methyl butyrate indicate that the inductive effect of Li^+ is stronger than that of Na^+ and that the ionic effect promotes less accumulation of negative charge on the carbonyl oxygen bound to Li^+. The $n \rightarrow \pi^*$ transition which is believed to be involved in McLafferty-type hydrogen rearrangement processes is shown to be energetically more favorable in Li^+ complexes compared to Na^+ complexes. This result is thus consistent with the experimental finding that loss of 1-butene occurs in Li^+ complexes and not in the corresponding Na^+ complexes of fatty acid *n*-butyl esters in low-energy collision-induced dissociation. (Int J Mass Spectrom 210/211 (2001) 21–30) © 2001 Elsevier Science B.V.

Keywords: Alkali adducts; Collision-induced dissociation; Fatty acids; Theoretical calculations

1. Introduction

With the development of desorption/ionization techniques such as fast atom bombardment (FAB), electrospray ionization and matrix-assisted laser desorption ionization alkali ion/molecule adducts are often observed in mass spectra or are generated by addition of alkali salts to introduce a charge center and allow mass spectrometric analysis. In recent studies we noted that Li^+ and Na^+ cationized fatty acid *n*-butyl esters show a very different fragmentation behavior in low- and high-energy collision-induced dissociations (CIDs) suggesting that the structure and electronic properties of the alkali com-

* Corresponding author. E-mail: claeys@uia.ua.ac.be

Dedicated to Professor Nico Nibbering on the occasion of his retirement.

1387-3806/01/$20.00 © 2001 Elsevier Science B.V. All rights reserved
PII S1387-3806(01)00409-2

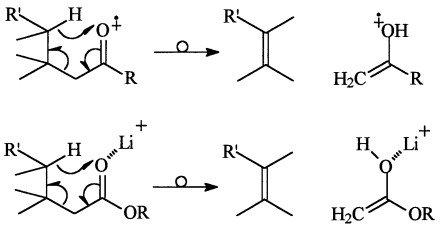

Scheme 1. Proposed mechanism for the McLafferty rearrangement observed for odd-electron molecular ions of ketones and esters and the McLafferty-type rearrangement observed for closed-shell Li^+ adducts of fatty acid *n*-butyl esters. R and R′ represent alkyl groups.

plexes affect the CID process [1,2]. It was found that Li^+ cationized fatty acid *n*-butyl esters lose 1-butene from the ester moiety in low-energy CID whereas the corresponding Na^+ complexes do not undergo this loss. Further, a very different fragmentation behavior was observed for Li^+ and Na^+ cationized fatty acid *n*-butyl esters in high-energy CID; whereas Li^+ complexes show exclusively charge-remote losses of elements of alkanes the Na^+ complexes reveal losses of both alkanes and alkyl radicals.

The loss of 1-butene from the ester part of Li^+ cationized fatty acid *n*-butyl esters observed in low-energy CID corresponds to a McLafferty-type rearrangement [3–5] (Scheme 1) which bears similarity with the well-known Norrish II photochemical rearrangement of ketones (intramolecular γ-hydrogen transfer process in triplet state photochemistry) [6–8].

A detailed understanding of photochemical reactions begins with an understanding of the manifold of excited state potential energy surfaces of the molecular species involved. Calculations at the ab initio level of the excited state hydrogen tunneling in the Norrish type II process were performed recently [9–11] and it was shown that the driving force in this process arises from the drastic change in electron reorganization around the oxygen atom that develops a large free valence in the lowest triplet state.

The molecular applications of density-functional theory (DFT) to excited states is based on the theorem that the energy of the lowest excited state of each symmetry may be obtained by minimizing a functional of its charge density [12]. From a formal point of view, the treatment of excited states in DFT is less well established than the treatment of ground states [13]. From a practical point of view, the ΔSCF (self-consistent field) method used in the present work is a well-established de facto method for treating simple types of excited states in DFT [13–15]. The gas phase reactivity of Li^+ toward neutral organic species and tetraphosphorous, P_4, has been investigated by both experimental and theoretical methods [16–20]. Li^+ has been shown to lead to very strong and mostly electrostatic interactions with neutral organic species [16–19] and to give rise to a stable P_4 ...Li^+ ion with a planetary structure in the gas phase [20]. Complexes between alkali metal acceptor ions and Lewis bases containing carbonyl functions such as formaldehyde complexes with Li^+ and Na^+ have been studied using ab initio calculations [21–24].

The present molecular orbital study of Li^+ and Na^+ cationized methyl and *n*-butyl esters as simple model compounds was undertaken in an attempt to rationalize the very different fragmentation behavior of Li^+ and Na^+ cationized fatty acid *n*-butyl esters with respect to the elimination of 1-butene from the ester moiety in low-energy CID. In particular emphasis is given to their excitation behavior because it is believed to be involved in low-energy CID processes. In addition to the excitation characteristics, general features of the structure, the nature of the bonding, dissociation energies and ionization potentials are also treated.

2. Computational details

The optimization of the geometry and the determination of the electronic properties of Li^+/Na^+ cationized methyl and *n*-butyl esters were carried out using version 3.4 of the Kohn-Sham module of the "densité de Montréal" suite of programs (deMon-KS), based upon the linear combination of Gaussian-type orbital Kohn-Sham DFT (LCGTO) [25–28]. Orbital basis sets of valence double zeta plus polarization quality were used: (621/41/1*) for C and O atoms, (621/1*/1+) for Li, (6321/411*/1+) for Na, and (41/1*) for H atoms. The deMon auxiliary basis sets [29] were as follows: (5,2;5,2) for C, (4,4;4,4) for 0, (4,3;4,3) for

Li, (5,4;5,4) for Na, and (5,1;5,1) for H atoms. Extended property analysis was performed using deMon properties [28] and visualized with Vu-334 graphics [30].

The geometries were optimized until both the norm of the local energy gradient and the norm of the maximal individual gradient fell below 0.0001 a.u. using the kinetic-energy-density dependent exchange-correlation scheme PLAP3 [31] and the GGA exchange-correlation functional of Perdew and co-workers PW91 [32,33]. Ab initio calculations were carried out at the MP2/6-31G* level using the GAMESS-UK package. For the simplest Li^+ cationized methyl acetate complex (**I**), optimized geometries in close agreement with MP2/6-31G* data were obtained (Table 1). The basis set superposition error for Li^+ bridging complexes was found to be insignificant (about 1 kcal/mol in the methyl acetate moiety and 0.03 kcal/mol in Li^+).

3. Results and discussion

3.1. Mass spectrometry observations

In previous studies we have examined the low- and high-energy CID of Li^+ and Na^+ cationized fatty acid *n*-butyl esters [1,2]. It was found that Li^+ cationized fatty acid *n*-butyl esters show the loss of 1-butene from the ester moiety in low-energy CID whereas the corresponding Na^+ complexes do not reveal this loss. Fig. 1 illustrates the low-energy CID spectrum of Li^+ cationized *n*-butyl palmitate. An ion at *m/z* 263 corresponding to the loss of 1-butene can clearly be observed in the spectrum of Li^+ cationized *n*-butyl palmitate but not in that of the Na^+ adduct (not shown), and, at higher magnification product ions formed by losses of alkanes and alkyl radicals which are characteristic of high-energy CID [1,2] are also observed. This loss of 1-butene from the ester moiety can be considered as a McLafferty-type rearrangement. Although the McLafferty rearrangement, which occurs in odd-electron molecular ions, has been investigated extensively [3,4] the McLafferty-type rearrangement in odd-electron molecular species such as protonated esters has only been studied to a limited extent [34]. It has been demonstrated that the conditions for a true McLafferty rearrangement, more specifically exclusive transfer of a δ hydrogen to the carbonyl group, are not fulfilled. *n*-Alkene losses from protonated esters, for example, have been shown to correspond to rather complex rearrangement reactions [34]. Since a $n \rightarrow \pi^*$ excited species is involved in the well-known Norrish II photochemical rearrangement of ketones which bears similarity with the McLafferty rearrangement it is logical to assume that a $n \rightarrow \pi^*$ transition may also be the trigger for the McLafferty-type rearrangement observed in low-energy CID of Li^+-cationized fatty acid *n*-butyl esters.

3.2. Geometry and energy

Previous theoretical calculations performed on methyl and *n*-butyl acetate revealed that the alkali ion complex of the Li^+ ion with these esters has two energetically favorable forms, a form with the lithium–oxygen bond co-linear with the ester carbonyl bond, and a form of the bidentate type (with the metal ion at equal distances (1.8 Å) from the two O atoms of the ester group in the case of the methyl acetate–Li^+ complex) which is less stable than the former [1]. Using ab initio calculations (MP2/6-31G* level with ZPVE correction) the linear form of the methyl acetate–Li^+ complex was found to be favored over the bidentate form by 1.3 kcal mol^{-1}. Further, it has been observed experimentally that the Na^+ complex of formaldehyde is also of the linear form [35]. Based on these results only the linear forms of Li^+ and Na^+ complexes were considered in the present study.

Due to the spatial orientation of the oxygen lone pair, the equilibrium location of the metal ion (M^+) in the lowest energy conformer was found to be co-linear with the C=O bond (at a distance of 1.81 and 2.16 Å for Li^+ and Na^+, respectively) (Fig. 2). The minimal optimized geometries for Li^+/Na^+ cationized methyl/*n*-butyl acetate and methyl butyrate are summarized in Table 1. These assignments of the preferred metal cation attachment site are consistent with data obtained from x-ray crystal structures of lithium and sodium enolates of tert-butyl methyl

Table 1
Optimized geometries and total energy of Li^+/Na^+ cationized methyl/*n*-butyl acetate and methyl butyrate (see Fig. 1 for definition of bonds in angstroms and angles in degrees)

Compound	$C_3H_6O_2$ PLAP/DFT	$C_3H_6O_2Li^+$**(I)** PLAP/DFT	$C_3H_6O_2Li^+$**(I)** PW91/DFT	$C_3H_6O_2Li^+$**(I)** MP2/6-31G*	$C_3H_6O^2Na^+$**(II)** PLAP/DFT	$C_4H_9COOCH_3$ PLAP/DFT	$C_6H_{12}O_2Li^+$**(III)** PLAP/DFT	$CH_3COOC_4H_9$ PLAP/DFT	$C_6H_{12}O_2Li^+$**(IV)** PLAP/DFT
C(1)–O(2)	1.461	1.475	1.475	1.508	1.473	1.471	1.503	1.461	1.478
O(2)–C(3)	1.375	1.323	1.328	1.341	1.330	1.372	1.316	1.377	1.323
C(3)–O(5)	1.221	1.255	1.262	1.279	1.248	1.222	1.258	1.222	1.254
O(5)–Me^+	...	1.805	1.817	1.766	2.155	...	1.797	...	1.814
C(3)–C(4)	1.516	1.507	1.507	1.504	1.510	1.518	1.509	1.524	1.514
Me^+O(5)C(3)	...	166.7	164.3	168.0	165.4	...	165.1	...	148.1
O(5)C(3)O(2)	123.7	122.7	124.3	124.3	123.9	124.0	122.9	123.1	124.2
C(3)O(2)C(1)		119.4	118.1	120.3	119.4	116.8	120.3	115.6	119.0
O(5)C(3)C(4)		123.9	122.2	124.3	123.9	125.1	124.1	126.2	124.2

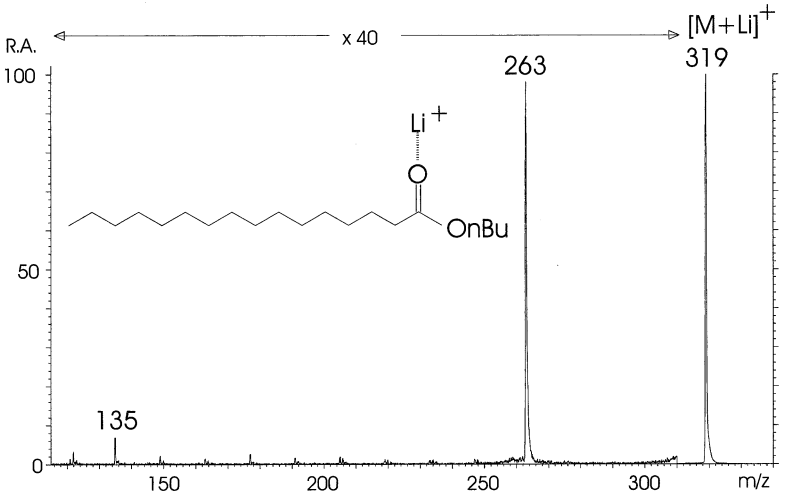

Fig. 1. Product ion spectrum obtained at low-energy collisional activation for Li^+ cationized *n*-butyl palmitate. The experimental conditions for FAB were the same as those reported in [1]. The spectrum was obtained on an Autospec-oa-TOF instrument (Micromass, Manchester, UK). The CID conditions were: E_{lab}=200 eV (E_{com}=2.5 eV); collision gas, helium; attenuation precursor ion beam, 50%.

ketone [36,37]. The average bond lengths of six crystallographically independent enols in a hexagonal prism-type crystal structure formed with alkali metal were found to be in the range of 1.85–1.95 and 2.24–2.33 Å for Li and Na, respectively. This relative difference of experimental bond lengths between Li and Na corresponds quite well with data from DFT calculations (Table 1). The geometry of the ester moiety undergoes a small change from its free state to the complex. It is worth noting that in the complexes C=O bond lengths are longer than that in the free ester, namely, 1.26 and 1.25 Å, for Li^+ and Na^+ complexes of methyl acetate, respectively (Table 1).

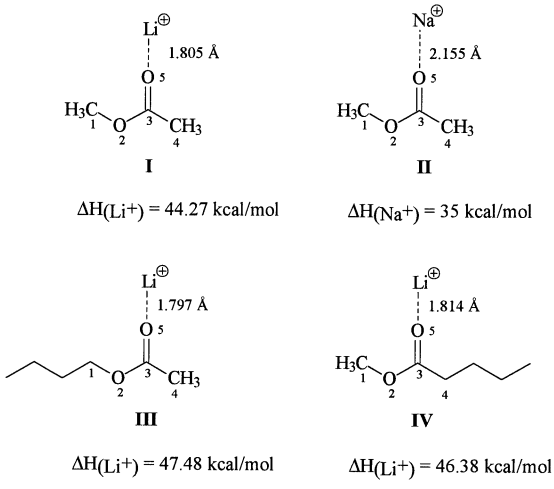

Fig. 2. DFT calculated Li^+/Na^+. . .O=C bond lengths and MA values of Li^+/Na^+ methyl/*n*-butyl acetate and methyl butyrate.

In order to better understand the factors governing the formation and stability of Li^+/Na^+ complexes in the gas phase we have calculated the metal affinity (MA). The MA is defined as the negative total energy change (ΔE) corresponding to the bond dissociation energy of the Lewis acid–metal complex (BM^+):

$$BM^+ \rightarrow B + M^+$$

$$\Delta E = E_{(BM+)} - (E_B + E_{M+})$$

The agreement between the PLAP/DFT and experimental MA for Li^+/Na^+ complexes with different Lewis bases (water, ammonia, and formaldehyde) is given in Table 2. The MA values calculated using PLAP/DFT for the Li^+/Na^+ cationized methyl/*n*-butyl esters (Table 2) indicate a greater stability of the Li^+ methyl acetate complex (**I**) (44.3 kcal/mol) than the corresponding Na^+ complex (**II**) (35.0 kcal/mol). The PLAP/DFT value of 1.80 Å for the Li^+...O bond of the $Li^+(H_2O)$ complex agrees quite well with the value of 1.85 Å calculated by Feller et al. [38] using

Table 2
MA of Li^+/Na^+ cationized esters calculated with PLAP/DFT

Compound	Calc. MA (kcal/mol)	Expt MA (kcal/mol)	Distance M^+–––O/N, (Å)
NH_3 Li^+	39.2	39.1[a]	2.04
H_2O Li^+	35.0	34.0[b]	1.80
		33.2 ± 1.9[c]	
HCOH Li^+	34.7	36.0[a]	1.82
$C_3H_6O_2$ Li^+ **(I)**	44.3	...	1.81
$C_6H_{12}O_2Li^+$ **(III)**	47.5	...	1.80
$C_6H_{12}O_2Li^+$**(IV)**	46.4	...	1.81
$C_3H_6O_2Na^+$**(II)**	35.0		2.16

[a]See [45].
[b]See [46].
[c]The value of 33.2 ± 1.9 kcal/mol obtained by Rodgers and Armentrout [17] is based on a direct measurement of the Li^+ (H_2O) bond energy using a CID method, whereas the other experimental MA values are based on indirect measurements using high pressure mass spectrometry. See [17].

high-level ab initio methods. The ion–molecule interaction (MA) can be discussed using a charge transfer term, an electrostatic term due to ion–molecular dipole interaction, and a polarization term arising from ion–induced dipole interaction.

3.3. Local atomic and molecular orbital properties

The charge transfer process involved in the formation of the alkali cationized esters as evaluated by Mulliken population analysis [q_A(Mull)] on the carbonyl oxygen shows a greater charge transfer in the case of Li^+ (8.340, 8.582, and 8.496 for free methyl acetate and its Li^+ and Na^+ complexes, respectively) (Table 3). Another type of analysis of local properties in real space was performed using the local softness *S*(Omega;) defined by the magnitude of the regional charge fluctuations λ(Omega;) in a region Omega; [39]. It can be seen from Table 3 that the oxygen atom (O5) in the Li^+ complex (**I**) shows a larger degree of electron localization in the ground state [smaller *S*(Omega;)] than the Na^+ complex (**II**). The inductive effect is less strong on more distant nuclei and the ionic effect promotes less accumulation of negative charge on the oxygen.

An alternative analysis of the molecular space is provided by the electron localization function (ELF) [40, 41] defined as

$$\mathrm{ELF} = 1/(1 + (D_\sigma/D^0_\sigma)^2$$

where D_σ represent the Fermi hole curvature defined at small interelectronic distance in the system, whereas $D°_\sigma$ is the analogous quantity for the homogenous electron gas with the same electron density (the ELF maps out the spatial probability of finding pairs of electrons). Being a scalar function in real space the ELF allows plots that reveal basin populations and regions of a higher or lower degree of electron localization corresponding to higher or lower local charge fluctuation [41]. The ELF scalar field maximum in terms of isolines (Fig. 3) shows nuclear core

Table 3
Atomic properties based on DFT wave functions

n	Compound		C(1)	O(2)	C(3)	C(4)	O(5)	Me
	$C_3H_6O_2$	*S*(Ω)	1.945	1.113	2.113	1.937	1.123	...
		q_A(Mull)	6.168	8.277	5.636	6.382	8.340	...
I	$C_3H_6O_2Li^+$	*S*(Ω)	1.917	1.1941	2.0443	1.9413	0.9867	0.0732
		q_A(Mull)	6.171	8.206	5.526	6.361	8.582	2.093
II	$C_3H_6O_2Na^+$	*S*(Ω)	1.921	1.176	2.044	1.940	1.054	0.112
		q_A(Mull)	6.175	8.219	5.548	6.363	8.496	10.111
	$C_4H_9COOCH_3$	*S*(Ω)	1.950	1.116	2.102	1.953	1.120	...
		q_A(Mull)	6.175	8.284	5.673	6.224	8.341	...
III	$C_4H_9COOCH_3Li^+$	*S*(Ω)	1.916	1.186	2.025	0.197	0.983	0.123
		q_A(Mull)	6.171	8.213	5.575	6.239	8.575	2.144
	$CH_3COOC_4H_9$	*S*(Ω)	1.962	1.123	2.133	1.936	1.120	...
		q_A(Mull)	5.994	8.289	5.632	6.399	8.346	...
IV	$CH_3COOC_4H_9Li^+$	*S*(Ω)	1.924	1.204	2.065	1.941	0.979	0.075
		q_A(Mull)	6.034	8.218	5.529	6.383	8.597	2.095

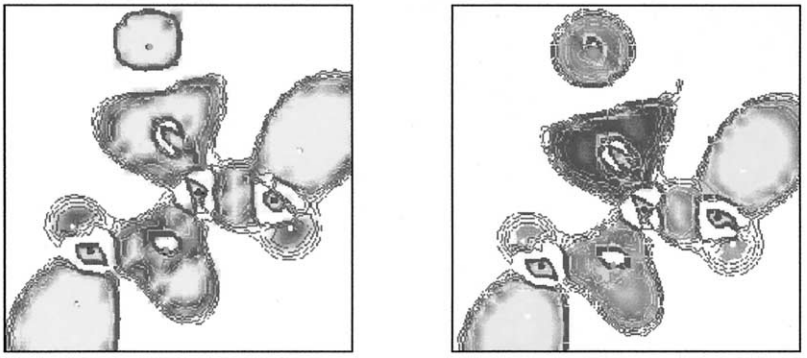

Fig. 3. DFT electron localization functions obtained for the Li^+(**I**) (left) and Na^+(**I**) (right) complexes.

interactions (very small around the atom nuclei), bonding interactions (well localized between bonded atoms as C=O, C–O, and C–C) and localization domains of lone pairs. The ELF obtained for the Li^+ complex (I) (Fig. 3, left) reveals the additional deformation of the oxygen lone pair localization domain around the Li^+ ion reflecting a larger degree of electron localization between the metal ion and the ester carbonyl function than in the case of the Na^+ complex (Fig. 3, right). This strong interaction between the ester carbonyl group and Li^+ cancels the repulsion between electrons localized in the region of the carbonyl function. As a consequence, the accommodation of incoming charge as well as radical formation is facilitated, processes which may be relevant for collision-induced dissociation.

The excitation behavior of the alkali-cationized esters was emphasized in this study because it is believed to be involved in the McLafferty-type rearrangement observed in low-energy CID of Li^+ cationized fatty acid *n*-butyl esters [1,2]. The electronic transitions can be described in terms of electron promotions between localized molecular orbitals (MOs) associated with the carbonyl group. The lone pair of electrons at the carbonyl oxygen in the complexes with Li^+ and Na^+ resides on the highest occupied MO (HOMO) orbital. The HOMO−1 of the Li^+ complex is the π orbital, whereas the lowest unoccupied MO (LUMO) is the π^* orbital. The LUMO+1 results from a σ-type interaction between Li^+ and the ester moiety and is localized mainly on Li^+(2*s*). This interaction in the Li^+/Na^+ complexes of methyl acetate (**I**, **II**) results in a systematic decrease of the orbital energies compared to the free ester (Table 4). The two-dimensional (*x*,*y*) contour plots of occupied (HOMO) and unoccupied 2*s* and 3*s* molecular orbitals of the Li^+ and Na^+ complexes are presented in Fig. 4.

By using the Hohenberg-Kohn-Sham density-functional theory it is possible to obtain the excitation energy at the ΔSCF level as a difference between total energies of the ground state and an excited configuration [12,13]. The unoccupied eigenfunctions are considered as virtual states and the excitation energies (E_{exc}^{TS}) are evaluated as differences of total energies of initial (ϵ_i) and excited states (ϵ_f) in which half an electron is transferred from the initial orbital to the final orbital:

$$E_{exc}^{TS} = \varepsilon_f^{TS} - \varepsilon_i^{TS}$$

The electronic transition of lowest energy resulting from a $n \rightarrow \pi^*$ promotion in the Li^+ complex (**I**) is

Table 4
Orbital energies and ionization potentials (eV)

Orbitals	CH_3COOCH_3	$CH_3COOCH_3Li^+$	$CH_3COOCH_3Na^+$
LUMO + 1	0.650	−5.949	−6.388
LUMO	−1.547	−6.555	−6.008
HOMO	−6.940	−12.257	−11.648
HOMO − 1	−7.834	−12.666	−12.148
HOMO − 2	−9.225	−13.504	−13.095
IP_{vert}(HOMO)	10.2 [a]	15.2	14.2

[a] IP_{exp}10.25 eV from [42].

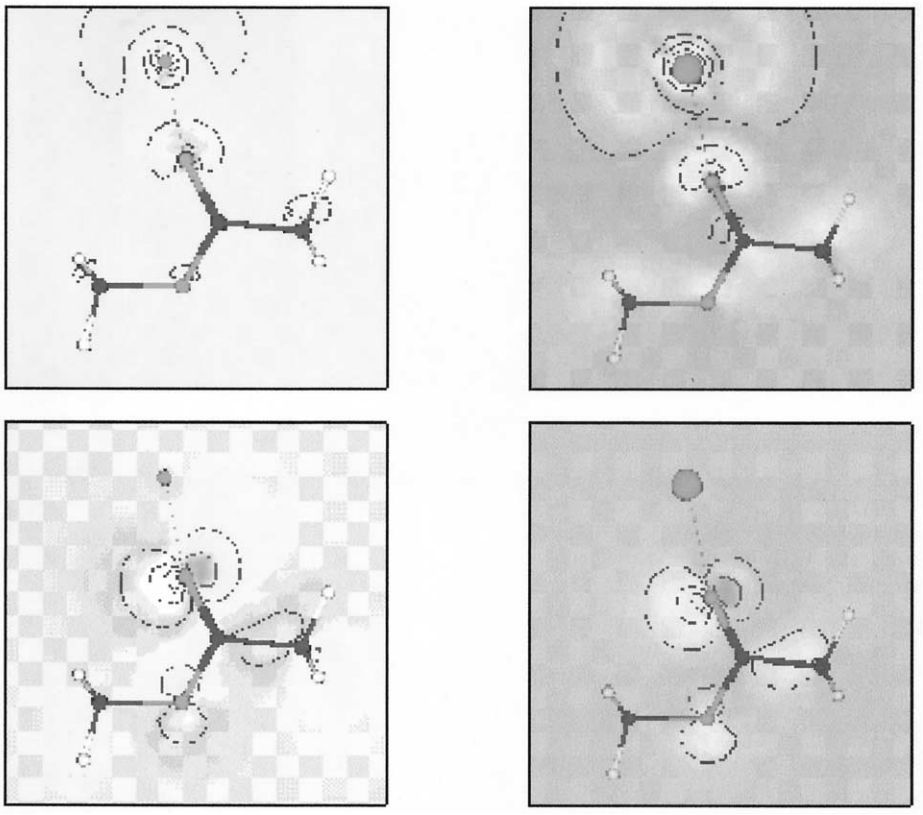

Fig. 4. Two-dimensional (x,y) contour plots for occupied (HOMO) and unoccupied 2s and 3s molecular orbitals of the Li^+(**I**) and Na^+(**I**) complexes. Left bottom: Li^+(**I**), HOMO (n); left top: Li^+(**I**), LUMO+1 (σ*); right bottom: Na^+(**I**), HOMO (n); right top: Na^+(**I**), LUMO (*sigma;*).

calculated to be 50304.8 cm^{-1}. Due to the considerable destabilization of the virtual π* orbital in the Na^+ complex the $n \rightarrow \pi$* transition requires a higher energy calculated as 56390.9 cm^{-1}.

We noted that the DFT (deMon) calculated value of the ionization potential of neutral methyl acetate evaluated as the difference between the total energy of the initial and the ionized state is in excellent agreement with the experimental one [42]. The calculated ionization potential of the Na^+ complex is lower than that of the Li^+ complex (Table 4).

The electronic transition $n \rightarrow \pi$* of neutral methyl acetate was calculated as 46476.8 cm^{-1} whereas the experimental one is at 210 nm or 47619 cm^{-1} [43]. The hypsochromic shift of the $n \rightarrow \pi$* transition in the case of cationized compounds (**I**) and (**II**) is due primarily to the inductive effect of the alkali metal ion which withdraws electrons from the carbonyl oxygen, causing the lone pair of electrons on oxygen to be held more firmly than in the absence of the metal ion. The inductive effect is stronger with Li^+ than with Na^+. The stronger the interaction is, the more stable is the "n" orbital and the greater the energy needed to promote an electron to the π* orbital.

Absorption of an energy quantum moves an electron from a given vibrational and rotational level within an electronic level to some vibrational and rotational level at the next or a higher electronic level. The energy acquired during a low-energy CID process may be of the same order of magnitude or higher than that of covalent bonds of the molecule and give rise to intermolecular abstraction of a hydrogen corresponding to a C–H bond energy of about 34000 cm^{-1}. We suggest that the $n \rightarrow \pi$* transition leads to McLaf-

ferty-type rearrangement processes upon deactivation of the electronically excited state in the gas phase involving cleavage of a C–H bond. In addition to $n \rightarrow \pi^*$ transitions electron promotions from the nonbonding 2*p* orbital of oxygen to Rydberg orbitals could also occur in carbonyl compounds [44]. Future research should clarify whether Rydberg excitations are the trigger for other collision-induced dissociation processes such as charge-remote fragmentation reactions.

4. Conclusions

Theoretical calculations performed in the present study on Li^+ and Na^+ cationized methyl and *n*-butyl acetate and methyl butyrate indicate that the inductive effect of Li^+ is stronger than that of Na^+ and that the ionic effect promotes less accumulation of negative charge on the carbonyl oxygen bound to Li^+. The $n \rightarrow \pi^*$ transition which is believed to be involved in McLafferty-type hydrogen rearrangement processes is shown to be energetically more favorable in Li^+ complexes compared to Na^+ complexes due to a significant destabilization of the π^* orbital in the latter. This result is thus consistent with the experimental finding that loss of 1-butene occurs in Li^+ complexes and not in the corresponding Na^+ complexes of fatty acid *n*-butyl esters in low-energy collision-induced dissociation.

References

[1] M. Claeys, L. Nizigiyimana, H. Van den Heuvel, I. Vedernikova, A. Haemers, J. Mass Spectrom. 33 (1998) 631.
[2] M. Claeys, L. Nizigiyimana, H. Van den Heuvel, P. J. Derrick, Rapid Commun. Mass Spectrom. 10 (1996) 770.
[3] F.W. McLafferty, Anal. Chem. 28 (1956) 306.
[4] F.W. McLafferty, Anal. Chem. 31 (1959) 82.
[5] F.P. Boer, T.W. Shannon, F.W. McLafferty, J. Am. Chem. Soc. 90 (1968) 7239.
[6] P.J. Wagner, B.-S. Park, Org. Photochem. 11 (1991) 227, and references therein.
[7] P.J. Wagner, Acc. Chem. Res. 4 (1971) 168.
[8] P.J. Wagner, Acc. Chem. Res. 6 (1983) 461.
[9] A.K. Chandra, V. Sreedhara Rao, Chem. Phys. Lett. 270 (1997) 87.
[10] M.V. Vener, S. Scheiner, J. Phys. Chem. 99 (1995) 642.
[11] Y. Niu, E. Christophy, P.J. Pisano, Y. Zhang, J.M. Hossenlopp, J. Am. Chem. Soc. 118 (1996) 4181, and references therein.
[12] R.G. Parr, W. Yang, Density Functional Theory of Atoms and Molecules, Oxford University Press, New York, 1989.
[13] R. Sing, B.M. Deb, Phys. Rep. 311 (1999) 47.
[14] F. Rogemond, H. Chermette, D. Salahub, Chem. Phys. Lett. 219 (1994) 228.
[15] R. Sing, G. Fronzoni, M. Stener, A. Lisini, P. Decleva, Chem. Phys. 210 (1996) 447.
[16] M.T. Rodgers, P.B. Armentrout, J. Mass Spectrom. 187 (1999) 359.
[17] M.T. Rodgers, P.B. Armentrout, J. Chem. Phys. 109 (1998) 1787.
[18] M.T. Rodgers, P.B. Armentrout, J. Phys. Chem. A 101 (1997) 1238.
[19] P. Burk, I.A. Koppel, I. Koppel, R. Kurg, J.-F. Gal, P.-C. Maria, M. Herreros, R. Notario, J.-L.M. Abboud, F. Anvia, R.W. Taft, J. Phys. Chem. A 104 (2000) 2824.
[20] J.-L.M. Abboud, I. Alkorta, J.Z. Davalos, J.-F. Gal, M. Herreros, P.-C. Maria, O. Mo, M.T. Molina, R. Notario, M. Yanez, J. Am. Chem. Soc. 122 (2000) 4451.
[21] H. Yang, Y.-H. Liau, T.-M. Su, J. Phys. Chem. 99 (1995) 177.
[22] H. Tachikawa, H. Murai, H. Yoshida, J. Soc. Faraday Trans. 89 (1993) 2369.
[23] B.J. McClelland, S. Norton, J. Mol. Struct., Theochem. 94 (1983) 299.
[24] F. Bernardi, G.F. Pedulli, J. Chem. Soc. Perkin II (1975) 194.
[25] A. St-Amant, D.R. Salahub, Chem. Phys. Lett. 169 (1990) 387.
[26] A. St-Amant, Ph.D. thesis, University of Montréal, DFT (LCGTO-) program deMon-KS, 1992.
[27] M.E. Casida, C. Daul, A. Goursot, A. Koester, L. Pettersson, E. Proynov, A. St-Amand, D. Salahub, H. Duarte, N. Godbout, J. Guan, C. Jamorski, M. Leboeuf, V. Malkin, O. Malkina, F. Sim, A. Vela, deMon Software, 1996.
[28] P. Calaminici, A.M. Koester, M. Leboeuf, A. Vela, deMon-Properties, version 3.0, Université de Montréal and THEOCHEM/Hannover, 1996.
[29] N. Godbout, D.R. Salahub, J. Andzelm, E. Wimmer, Can. J. Chem. 70 (1992) 560.
[30] B. Ozell, F. Guibalt, R. Camarero, R. Magnan, in Computer Graphics and Flow Visualization in Computational Fluid Dynamics, G. Degrez, H. Deconinck (Ed.), Lecture Series 1991-10, von Karman Institute for Fluid Dynamics, Rhode Saint-Genèse, Belgium, 1991.
[31] E.I. Proynov, S. Sirois, D.R. Salahub, Int. J. Quant. Chem. 4 (1997) 427.
[32] J.P. Perdew, J.A. Chevary, S.H. Vosko, K.A. Jackson, M.R. Pederson, D.J. Singh, C. Fiolhais, Phys. Rev. B 46 (1992) 6671; erratum, ibid. 48 (1993) 4976.
[33] J.P. Perdew, K. Burke, Y. Wang, Phys. Rev. B 54 (1996) 16544.
[34] M. Zollinger, J. Seibl, Org. Mass Spectrom. 20 (1985) 649.
[35] J.H. Callomon, E. Hirota, K. Kuchitsu, W.J. Lafferty, A.G. Maki, C.S. Pote, Structure Data on Free Polyatomic Molecules, Landolt-Bornstein, Numerical Data and Function Rela-

tionships in Science and Technology, New Series, K.H. Hellwege (Ed.), Springer, Berlin, 1976, Vol. 7.
[36] P.G. Williard, G.B. Carpenter, J. Am. Chem. Soc. 107 (1985) 3345.
[37] P.G. Williard, G.B. Carpenter, J. Am. Chem. Soc. 108 (1986) 462.
[38] D. Feller, E.D. Glendening, R.A. Kendall, K.A. Peterson, J. Chem. Phys. 100 (1994) 4981.
[39] N. Neshev, E. Proynov, T. Mineva, Bulg. Commun. Chem. 30 (1998) 488.
[40] D. Seebach, H.M. Burger, D.A. Plattner, R.T. Nesper Fassler, Helv. Chim Acta 76 (1993) 2581.
[41] W. Davies, W.A. Noyes Jr., J. Am. Chem. Soc. 69 (1947) 2153.
[42] P.H. Cannington, N.S. Ham, J. Electron Spectrosc. Relat. Phenom. 36 (1985) 203.
[43] E.S. Stern, C.J. Timmons, Electronic Absorption Spectroscopy in Organic Chemistry, Edward Arnold, London, 1970, p. 227.
[44] C.M. Haddad, J.B. Foresman, K.B. Wiberg, J. Phys. Chem. 97 (1993) 4293.
[45] R.L. Woodin, J.L. Beauchamp, J. Am. Chem. Soc. 100 (1978) 501.
[46] I. Dzidic, P. Kebarle, J. Phys. Chem. 74 (1970) 1466.